Received: 21 February 2025 | Revised: 24 October 2025 | Accepted: 19 November 2025

DOI: 10.1111/bph.70301

RESEARCH ARTICLE

A PK/PD study on antihyperalgesia by an α2/3-GABA$_A$ receptor PAM in mice: Lack of tolerance liability and potential involvement of γ1-GABA$_A$ receptors

Elena Neumann[1,2] | Mariana O. Popa[3] | Karen T. Elvers[3] | Misa Oyama[1] | Daniel Ulrich[1] | Marcus Hanley[3] | Gui Jie Feng[3] | Thomas Hathaway[3] | William T. Ralvenius[1] | Thomas Grampp[1] | Dietmar Benke[1] | John R. Atack[3] | Hanns Ulrich Zeilhofer[1,4]

[1]Institute of Pharmacology and Toxicology, University of Zurich, Zurich, Switzerland

[2]Department of Anesthesiology, University Hospital Zurich, Cambridge, Massachusetts, USA

[3]Medicines Discovery Institute, Cardiff University, Cardiff, UK

[4]Institute of Pharmaceutical Sciences, Swiss Federal Institute of Technology (ETH) Zurich, Zurich, Switzerland

Correspondence
Dr. Hanns Ulrich Zeilhofer, Institute of Pharmacology and Toxicology, University of Zurich, Winterthurerstrasse 190, CH-8057 Zurich, Switzerland.
Email: zeilhofer@pharma.uzh.ch

Funding information
The work was partially supported by grants from the Deutsche Forschungsgemeinschaft (NE 2126/1-1) to EN and the Clinical Research Priority Program 'Pain – from phenotypes to mechanism' of the Faculty of Medicine, University of Zurich, to HUZ. Work conducted at the Medicines Discovery Institute was supported by MRC Grant MR/S019162/1 to JRA.

Abstract

Background and Purpose: GABA$_A$ receptors (GABA$_A$Rs) are heteropentameric ion channels that control almost all CNS functions, including spinal nociception. Most GABA$_A$Rs contain a γ2 subunit but differ in their α and β subunit composition. TPA023B is an α2/α3 subtype selective, non-sedative, positive allosteric modulator (PAM) with antihyperalgesic activity in rodents. The pharmacokinetic/pharmacodynamic (PK/PD) characteristics of its antihyperalgesic action are unknown.

Experimental Approach: To establish the PK/PD relationship for the antihyperalgesic effects of TPA023B, blood and brain concentrations, and brain and spinal cord receptor occupancies (RO) were determined at various time points following the administration of single oral doses of TPA023B in mice, and correlated with the antihyperalgesic effects (increases in paw withdrawal thresholds to punctate mechanical stimuli). In addition, the potentiating effects of TPA023B on recombinant γ1- and γ2-containing GABA$_A$Rs (γ1-GABA$_A$Rs and γ2-GABA$_A$Rs, respectively) were determined in electrophysiological (patch-clamp) and fluorometric (membrane potential-sensitive dye) assays.

Key Results: Antihyperalgesic effects of TPA023B correlated well with blood and brain concentrations, and no signs of tolerance (clockwise hysteresis) were observed. However, antihyperalgesia did not correlate with receptor occupancy at γ2-GABA$_A$Rs, suggesting that a relevant part of the antihyperalgesic action occurred through non-γ2-GABA$_A$Rs. In this regard, experiments in heterologous expression systems revealed that TPA023B not only potentiates γ2 but also γ1 containing GABA$_A$Rs.

Abbreviations: AUC, area under the curve; BDZ, benzodiazepine; CCI, chronic constriction injury; FLIPR, fluorometric imaging plate reader; MPE, maximum possible effect; PAM, positive allosteric modulator; PK, pharmacokinetic; PD, pharmacodynamic; RO, receptor occupancy.

Conclusions and Implications: Antihyperalgesic effects of TPA023B do not undergo tolerance development. Besides γ2-GABA$_A$Rs, γ1-GABA$_A$Rs appear to contribute to the antihyperalgesic effects of TPA023B. γ1-GABA$_A$R selective PAMs may hence have a therapeutic potential in chronic pain conditions.

KEYWORDS
analgesia, hysteresis, PK/PD model, proteresis, receptor occupancy, TPA023B

1 | INTRODUCTION

Chronic pain is a debilitating medical condition affecting about 20% of humans (Breivik et al., 2006). Plastic changes in neuronal communication within the spinal dorsal horn are major contributors to chronic pain states. Among them, a reduced inhibitory tone by GABAergic neurons plays a particular role both in neuropathic and inflammatory conditions (for reviews, see De Koninck, 2007; Zeilhofer & Zeilhofer, 2008; Zeilhofer et al., 2012). Restoring a physiological level of inhibition with **GABA$_A$ receptor** (GABA$_A$R) positive allosteric modulators. (PAMs) should therefore constitute a rational approach to the treatment of chronic pain (Zeilhofer et al., 2012; Zeilhofer et al., 2015).

GABA$_A$Rs are heteropentameric receptor complexes. A total of 19 genes encode GABA$_A$R subunits. Most GABA$_A$Rs in the CNS contain two α, two β and one γ subunit chosen from a repertoire of 6 α (α1–α6), 3 β (β1–β3), and 3 γ (γ1–γ3) subunits (Sieghart & Savic, 2018). The great majority of GABA$_A$Rs in the CNS contain a γ2 subunit, which together with an α1, α2, α3, or α5 subunit forms the high affinity benzodiazepine (BDZ) binding site. α4 and α6 subunits cannot form a high affinity BDZ binding site because of the presence of a histidine to arginine amino acid exchange in their N-terminal extracellular domain. Positive allosteric modulation of GABA$_A$Rs that contain an α1 subunit induces sedation and anticonvulsive actions (Rudolph et al., 1999). Conversely, potentiation of GABA$_A$Rs containing α2 and/or α3 subunits elicits profound anxiolytic effects in the absence of sedation (Dias et al., 2005; Löw et al., 2000), as well as antihyperalgesic (Knabl et al., 2008; Lorenzo et al., 2020; Ralvenius et al., 2015) and antipruritic effects (Ralvenius et al., 2018). Indeed, the prototypic α2/α3-GABA$_A$R PAM TPA023 demonstrated anxiolytic-like activity in a Phase 2 study of generalised anxiety disorder (Atack, 2009). TPA023B, the back-up compound to TPA023, is another positive allosteric modulator (PAM) at GABA$_A$Rs containing α2 and/or α3 subunits (Atack, 2011) that also binds to the high affinity BDZ binding site (Ralvenius et al., 2018). It has no activity at α1 GABA$_A$Rs and only relatively weak activity at α5 GABA$_A$Rs. TPA023B possesses anxiolytic activity in rodents, non-human primates and humans (Atack et al., 2011), and is, in addition, antihyperalgesic in various mouse pain models, where it reduces both the sensory and the affective component of pain (Neumann et al., 2021). This antihyperalgesic efficacy corresponds well with the enrichment of α2 and α3 GABA$_A$R subunits in the spinal dorsal horn (Paul et al., 2012), where somatosensory, including nociceptive, processing occurs. Dorsal horn GABA$_A$R expression is also somewhat peculiar as about 20% of the total GABA$_A$R γ subunit mRNA encodes for the γ1 subunit (Neumann et al., 2024), which is expressed only at very low levels in most supraspinal CNS regions (Pirker et al., 2000). Although the antihyperalgesic effects of TPA023B and of similar compounds are well established, detailed information about the required CNS concentrations and levels of receptor occupancies (RO) are unknown. To address these questions, we have conducted this pharmacokinetic/pharmacodynamic (PK/PD) study on the antihyperalgesic actions of TPA023B.

Our results reveal, over the dose range tested, a good correlation of whole blood and brain concentrations of TPA023B with the degrees of antihyperalgesia achieved. Plots of antihyperalgesic activity over time-dependent drug concentrations in the brain showed counterclockwise—rather than clockwise—hysteresis, indicating that, unlike the sedative effects of conventional non-selective BDZ site agonists, antihyperalgesia by TPA023B does not undergo tolerance development. An unexpected finding was that the degree of RO determined with the γ2/γ3 GABA$_A$R selective radioligand [^{3}H]flumazenil did not correlate with the antihyperalgesic activity, suggesting that other (non-γ2/γ3 containing) GABA$_A$Rs make a relevant

What is already known?

- Subtype selective positive allosteric modulators of GABA$_A$ receptors (GABA$_A$Rs PAMs) exert antihyperalgesic effects in rodent models of chronic pain.
- TPA023B is an α2/α3 subtype selective, non-sedative, GABA$_A$R PAM

What does this study add?

- These antihyperalgesic effects do not undergo tolerance development and are likely mediated by non-canonical (γ1-)GABA$_A$Rs.

What is the clinical significance?

- γ-1 GABA$_A$Rs may be new potential targets for analgesic drugs.

contribution to antihyperalgesia. In line with this finding, experiments on recombinant $GABA_AR$s showed that TPA023B not only potentiates γ2-$GABA_AR$s but also γ1-$GABA_AR$s.

2 | METHODS

2.1 | General study design

We first measured antihyperalgesic effects of different doses of TPA023B in the chronic constriction model of neuropathic pain in mice. We then obtained blood and brain concentrations of TPA023B to obtain basic pharmacokinetic (PK) parameters of TPA023B in mice and to correlate antihyperalgesic effects with drug concentrations. To examine whether a potential loss of efficacy during drug exposure following a single dose of TPA023B occurs, we made hysteresis plots of time-dependent anti-allodynic effects versus time-dependent drug concentrations in blood and brain. A chronic 9-day treatment experiment was performed to test whether the antihyperalgesic action of TPA023B would undergo tolerance development during repeated drug exposure. Receptor occupancy was measured in brain and spinal cord to correlate RO with antihyperalgesic effects of TPA023B. Finally, we analysed the binding of TPA023B to $GABA_AR$s containing either γ1 or γ2 subunits and its modulatory effects on these receptors in heterologous expression systems. The authors have followed the recommendations set out in the *British Journal of Pharmacology* (*BJP*) editorials where they are relevant.

2.2 | Mice

Experiments were performed in wild-type mice of the 129X1/SvJ background. This strain was chosen to allow comparisons with previous work from our group.

Breeding pairs of mice were obtained from The Jackson Laboratories and were bred in-house. Permission for animal experiments was obtained from the Canton of Zürich (license numbers ZH096/2021 and ZH034/2024). Mice were randomly attributed to the different treatment doses and, when applicable, to the different time points. The study has no implication for the 3R principles. All experiments were performed in 7- to 10-week-old male and female mice. Mouse weight was 20.63 ± 0.19 g (range 17–25 g, $n = 30$) and 25.13 ± 0.23 g (range 19–28 g, $n = 46$) for female and male mice, respectively. Animal studies are reported in compliance with the ARRIVE guidelines (Percie du Sert et al., 2020) and with the recommendations made by the *British Journal of Pharmacology* (Lilley et al., 2020). Mice were kept under specific pathogen free (conditions in type T2L cages with 2–6 mice per cage with a regular 12/12 h light/dark cycle at room temperature (21–24°C) and at 40–60% humidity with *ad libitum* access to food and water. Trunk wood (Safe Aspen Premium Hygiene) was used as bedding material. Environmental enrichment included paper crinkles (ARBOCEL crinklets natural) and paper tissue (Kleenex). In-house breeding was performed through 1:1 matings. All experiments were performed during the light phase. Well-being of mice in experiments was checked every day. Termination criteria (humane endpoints) included infected or open wounds, signs of paralysis, signs of autotomy behaviour, weight loss > 10%, strongly ruffled fur, permanently closed eyes, arced back or severely reduced spontaneous activity during any stage of the experiment.

2.3 | Drugs

TPA023B (6,2′ -difluoro-5′- [3-(1-hydroxy-1-methylethyl)imidazo [1,2-b][1,2,4]triazin-7-yl]biphenyl-2-carbonitrile) was synthesised by PharmaBlock Sciences (Nanjing), Inc. China (cat # PBLJB817). For oral (po) administration, TPA023B was suspended in 0.9% saline (sodium chloride, Sigma-Aldrich, St. Louis, MO, USA) and 1% Tween 80 (Sigma-Aldrich). For in vitro functional experiments (i.e. electrophysiological and fluorescence-based assays), TPA023B was dissolved in dimethyl sulfoxide (DMSO, Sigma-Aldrich; final concentration < 0.1%) and subsequently diluted in appropriate assay buffer.

2.4 | Chronic constriction injury surgery

Neuropathic pain was induced by applying a chronic constriction injury (CCI; Bennett & Xie, 1988) to the left sciatic nerve proximal to the trifurcation with three loose (5–0, not absorbable) silk (Ethicon, Somerville, NJ, USA) ligatures in mice anesthetised with isoflurane at 1–3%. Skin was closed with 5–0 Dermalon sutures (Covidien, Minneapolis, MN, USA). Care was taken to ensure aseptic conditions. This CCI model is a standard rodent model of neuropathic pain and well established in mice.

2.5 | Behavioural experiments

The effects of TPA023B on mechanical hyperalgesia were assessed between 7 and 10 days after surgery, except in the tolerance experiments, in which pain thresholds were assessed for up to 14 days after surgery. Electronic von Frey filament (no. 7; IITC, Woodland Hills, CA, USA) was used to determine mechanical withdrawal thresholds. Three measurements were taken per time point and mouse. Mice were culled by decapitation in deep isoflurane anaesthesia at the end of the experiment. The percent maximal possible effect (%MPE) was calculated as follows:

$$\%\mathrm{MPE}(t) = \left(\left(W(t) - W_{\mathrm{predrug}}\right)/\left(W_{\mathrm{preCCI}} - W_{\mathrm{predrug}}\right)\right) \times 100\% \quad (1)$$

where $W(t)$ is the paw withdrawal thresholds at time point t, W_{predrug} is the withdrawal threshold measured after CCI surgery but before TPA023B application and W_{preCCI} is the baseline withdrawal threshold before CCI surgery.

2.6 | Whole blood and brain concentrations of TPA023B

2.6.1 | Sample collection

Mice were treated with TPA023B (0.1, 0.3 and 1.0 mg kg^{-1}, p.o.) and culled by decapitation in deep isoflurane anaesthesia at 0.5, 1, 1.5, 2, 3, 4, 5, 6, 10 and 24 h post drug administration. At these points, blood and CNS samples (cerebrum, cerebellum and spinal cord), snap frozen separately on dry ice, were taken for both PK and RO analyses (see Section 2.6). Three mice (two male and one female) were analysed per time point.

2.6.2 | Blood preparation

Whole blood concentrations were obtained using a dried blood spot method (Deglon et al., 2011). In brief, 10 µL of whole blood collected after decapitation was spotted directly onto filter paper (Thermo Fisher Scientific, Waltham, MA, USA, Cat no 84783) and allowed to dry overnight at room temperature. All samples were extracted into 0.5 mL MeOH containing internal standard (carbamazepine) and then vacuum evaporated. The same procedure was applied to matrix matched standard curve samples.

2.6.3 | Brain preparation

One hemisphere was thawed, weighed and homogenised to 100 mg mL^{-1} in ice cold 10 mM K_2PO_4 (pH 7.0). One hundred microlitres of homogenised sample or matrix matched standard curve sample was then precipitated in 900 µL methanol containing internal standard (carbamazepine).

2.6.4 | Analytics

The dried blood and brain samples were then re-suspended in 50% acetonitrile. The levels of compound in blood and brain were analysed using mass spectrometry (Waters, Milford, MA, USA, Xevo TQ-S micro). Analyte standard curve samples (matrix matched in untreated mouse blood and then spotted onto filter paper or matrix matched in untreated mouse brain homogenate) and dry blood spot papers or brain samples from treated mice were precipitated in methanol containing an internal standard (carbamazepine). Once centrifuged, the supernatant was diluted and subjected to HybridSPE filtration to remove lipids to minimise matrix associated ion suppression during MS analysis, followed by vacuum evaporation. The dried samples were then re-suspended in 50% acetonitrile and analysed via LC/MS–MS. Analyte peak areas were normalised to the internal standard, and concentrations interpolated from the matrix matched standard curve.

2.7 | Receptor occupancy

RO was determined ex vivo by the level at which TPA023B inhibited binding of the radioligand [^{3}H]flumazenil to the $GABA_AR$ BDZ binding site (Li et al., 2006). On the day of assay, each tissue sample was rapidly homogenised in 8× volumes (brains) or 20× volumes (spinal cord) of ice-cold assay buffer (10 mM potassium phosphate buffer, pH 7.4). For brains, 300 µL aliquots from each sample was added to 1050 µL of assay buffer and 150 µL of [^{3}H]flumazenil (final concentration of 4 nM). For spinal cords, 100 µL aliquots from each sample were added to 400 µL assay buffer containing 2.5 nM [^{3}H]flumazenil.

A reference compound, bretazenil, was added ex vivo to a group of samples from vehicle dosed mice to block all BDZ binding sites in order to define the level of non-specific binding of [^{3}H]flumazenil. For spinal cord, nonspecific [^{3}H]flumazenil binding was in addition determined with samples derived from mice that had been injected with 5 mg kg^{-1} (i.p.) bretazenil (dissolved in PEG300) to completely occupy all BDZ-binding sites. All samples were vortexed immediately and incubated for 20 s on ice. The incubations were terminated by filtration through Whatman GF/B filters and washing with 10 mL of ice-cold 50 mM Tris buffer (pH 7.4). The radioactivity retained on the filters was determined by liquid scintillation counting using a Packard TriCarb2500 or TriCarb2900 Liquid Scintillation Analyser.

For each dosed mouse, triplicate samples were analysed (the membrane-bound radioactivity counted) and the results averaged. The value of non-specific binding defined using bretazenil was subtracted to give values of specific binding. The percent $GABA_A$ RO of the test compound at a specific dose and treatment time was calculated as the percentage by which the specific binding (radioactivity) observed in the vehicle-treated group was inhibited by drug as measured in the drug-treated rodents (Li et al., 2006). Therefore, the percentage RO of TPA023B in drug-treated animals was expressed as

$$\begin{aligned} RO = 100 - \big(\big(CPM_{sample} - CPM_{bretazenil\ control}\big)/ \\ \big(CPM_{vehicle\ control} - CPM_{bretazenil\ control}\big) \times 100\%\big). \\ CPM = counts\ per\ minute \end{aligned} \quad (2)$$

2.8 | Pharmacokinetic/pharmacodynamic (PK/PD) modelling

2.8.1 | Whole blood and brain concentrations over time

Whole blood and brain concentrations of TPA023B over time ($c(t)$) after oral drug administration were fitted to the Bateman function:

$$c(t) = A1 \times (k_{a1}/(k_{a1} - k_{e1}) \times (\exp(-k_{e1} \times t) - \exp(-k_{a1} \times t)) \quad (3)$$

where A1 is the arbitrary constant, k_{a1} is the rate constant of drug absorption into whole blood or brain, k_{e1} is the rate constant of

drug elimination from whole blood or brain, and t is the time after drug administration.

2.8.2 | Drug effect versus time

Drug effect (percent maximum possible antihyperalgesia) was plotted versus time. Data were fitted to the Hill equation:

$$E(c_{\text{effect}}(t)) = E_{\max} / \left(1 + (c_{\text{half}} / c_{\text{effect}}(t))^{nH}\right), \quad (4)$$

with an embedded Bateman function describing the time course of the concentration of TPA023B in the (unknown) effect compartment:

$$c_{\text{effect}}(t) = A2 \times (k_{a2} / (k_{a2} - k_{e2})) \times (\exp(-k_{e2} \times t) - \exp(-k_{a2} \times t)) \quad (5)$$

where A2 is the arbitrary factor, k_{a2} is the rate constant for absorption into the effect compartment, k_{e2} is the rate constant for elimination from effect compartment, and t is the time after drug administration.

Terminal half-life of TPA023B was estimated from the k_e values obtained in the various fits:

$$t_{1/2} = \ln 2 / k_e \quad (6)$$

2.8.3 | Drug effect versus whole blood or brain concentrations (hysteresis plots)

To detect potential hysteresis effects between antihyperalgesia and whole blood or brain concentrations, drug effects (percent maximum possible antihyperalgesia) measured at time point t ($E(t)$) were plotted against measured drug concentrations at the same time point in whole blood or brain ($c(t)$). Data points in the graphs were overlaid with curves that display the fits of $E(t)$ to Equation (4) plotted versus fits of $c_{\text{blood}}(t)$ or $c_{\text{brain}}(t)$ from Equation (3).

2.8.4 | Dose–response curves

Dose–response curves were calculated for the maximum degree of antihyperalgesia reached for a particular dose and for the areas under the effect-versus-time curve (AUC). AUCs were calculated from the fits of $E(t)$ to the Bateman function by numerical integration over time using the trapezoid method. The dose response data were fitted to the Hill equation.

$$E(D) = E_{\max} / \left(1 + (D_{\text{half}} / D)^{nH}\right) \quad (7)$$

where D_{half} is the dose at which the half-maximal effect is reached, nH is the Hill coefficient, and D is the dose administered.

2.8.5 | RO versus time

RO values (RO(t)) were plotted against time. Data were fitted to the Hill equation:

$$\text{RO}\,(c_{\text{effect}}(t)) = \text{RO}_{\max} / \left(1 + (c_{\text{half}} / c_{\text{effect}}(t))^{nH}\right) \quad (8)$$

with an embedded Bateman function describing the time course of the (unknown) concentration of TPA023B in the effect compartment:

$$c_{\text{effect}}(t) = A4 \times (k_{a4} / (k_{a4} - k_{e4})) \times (\exp(-k_{e4} \times t) - \exp(-k_{a4} \times t)) \quad (9)$$

where $\text{RO}_{\max}$ is the maximal RO with the given dose, c_{half} is the brain drug concentration yielding half-maximal RO, nH is the Hill coefficient, A4 is the arbitrary factor; k_{a4} is the rate constant for absorption into the effect compartment, k_{e4} is the rate constant for elimination from the effect compartment, and t is the time after drug administration.

2.8.6 | RO versus dose

$$\text{RO}(D) = \text{RO}_{\max} / \left(1 + (D_{\text{half}} / D)^{nH}\right) \quad (10)$$

where D_{half} is the dose at which the half-maximal RO is reached, nH is the Hill coefficient, and D is the dose administered. $\text{RO}_{\max}$ was set to 100%.

2.8.7 | RO versus c_{brain}

$$\text{RO}\,(c_{\text{brain}}) = \text{RO}_{\max} / \left(1 + (c_{\text{half}} / c_{\text{brain}})^{nH}\right) \quad (11)$$

where D_{half} is the dose at which the half-maximal RO is reached, nH is the Hill coefficient, and c_{brain} is the concentration in the brain. $\text{RO}_{\max}$ was set to 100%.

2.8.8 | Antihyperalgesia versus time-dependent receptor occupancy (RO) (hysteresis plots)

To detect potential hysteresis between antihyperalgesia and RO, measured percent maximal possible antihyperalgesia values at time point t ($E(t)$) were plotted against RO(t). Data points in the graphs were overlaid with the curve, which displays the fitted E ($c_{\text{effect}(t)}$) from Equation (4) plotted versus the fitted RO(t) from Equation (8).

2.8.9 | Receptor occupancy (RO) versus time-dependent brain concentrations (hysteresis plots)

To detect potential hysteresis effects between RO and brain concentrations, RO measured at time point t (RO(t)) was plotted against the measured concentration in brain at the same time point ($c_{\text{brain}}(t)$).

Graphs were overlaid with the curves in which the fitted RO(t) (Equation 8) was plotted versus the fitted $c_{brain}(t)$ from Equation (3).

2.9 | Electrophysiology

The effects of TPA023B on currents through recombinant $GABA_A$Rs were studied in HEK293 cells (ATCC; RRID: CVCL_0045) transiently transfected with rat $GABA_A$R subunits using Lipofectamine™ 2000 (Invitrogen, Waltham, MA, USA). To ensure expression of the γ1 or γ2 subunit in all recorded cells, a plasmid was used for γ1 and γ2 subunit expression that also contained an IRES eGFP expression cassette. Only cells with green fluorescence were selected for recording. The transfection mixture contained in (μg): 1 α2, 1 β3, 3 γ1-eGFP or γ2-eGFP. This subunit combination was chosen because antihyperalgesia by BDZ site agonists occurs mainly through α2 $GABA_A$Rs (Knabl et al., 2008) and because the α2 subunit is most frequently associated with β3 subunits (Benke et al., 1994).

Whole-cell patch-clamp recordings were made at room temperature (20–24°C) at a holding potential of −60 mV 18–48 h after transfection. Recording electrodes were filled with intracellular solution containing (in mM): 120 CsCl, 10 EGTA, 10 HEPES (pH 7.40), 4 $MgCl_2$, 0.5 GTP and 2 ATP. The external solution contained (in mM): 150 NaCl, 10 KCl, 2.0 $CaCl_2$, 1.0 $MgCl_2$, 10 HEPES (pH 7.40) and 10 glucose. GABA at EC_{10} together with various concentrations of TPA023B was applied for 2–10 s using a manually controlled application system. EC_{10} values of GABA were 0.87 and 1.16 μM for γ1 and γ2 containing $GABA_A$Rs, respectively. EC_{50} values and Hill coefficients (nH) were obtained from fits of normalised concentration–response curves to the Hill equation

$$I_{GABA} = I_{max}\,[GABA]^{nH} / \left([GABA]^{nH} + [EC_{50}]^{nH}\right). \quad (12)$$

I_{max} was determined as the average maximal current elicited by a saturating concentration of 1 mM GABA. TPA023B was dissolved in DMSO (final concentration < 0.1%) and subsequently diluted in external solution and co-applied with GABA without preincubation. Potentiation was calculated as

$$E(c) = (I(c) - I_0)/I_0 \times 100\% \quad (13)$$

2.10 | Fluorometric imaging plate reader (FLIPR) assay

The potentiating actions of TPA023B in comparison to the canonical BDZ site agonist diazepam were evaluated using the FLIPR membrane potential assay in the FLIPR Penta system (Molecular Devices, San Jose, CA, USA). TPA023B was tested for its ability to modulate ion channels through an increase in fluorescent signal as cellular membrane potential changes. For the FLIPR assays, a stable HEK293 cell line expressing α2β3γ1$GABA_A$Rs (HEK-α2β3γ1) and an inducible human Ltk(−) cell line (ATCC; RRID: CVCL_3392) expressing α2β3γ2$GABA_A$ (Ltk-α2β3γ2) were used.

Cells expressing α2β3γ1 were maintained in Dulbecco's Modified Eagle Medium (DMEM) medium supplemented with 10% fetal bovine serum tetracycline-free 1% L-glutamine, 0.6 mg mL^{-1} geneticin, 4 μg mL^{-1} blasticidin, 0.4 mg mL^{-1} zeocin and 1× non-essential amino acids. Cells expressing α2β3γ2 were maintained in DMEM F1/2 with 10% fetal bovine serum, 1% penicillin/streptomycin and 1 mg mL^{-1} geneticin. Both cell lines were maintained at 80% confluence. Black walled, clear bottom 384-well assay plates were coated with poly-D-lysine (PDL) overnight. The PDL solution was removed, and the plates were washed twice with sterile water and left to dry completely.

The cell seeding density was optimised so that a uniform 90% confluent monolayer was formed on the day of the assay. Both cell lines were seeded into poly-D-lysine coated plates at 10,000 cells per well in 50 μL culture media. Seeded plates were incubated at 37°C in a humidified atmosphere with 5% CO_2. After 24 h, expression in Ltk(−) cells was achieved by incubating the cells in media containing dexamethasone at a final concentration of 300 nM and incubated further at 18–24 h prior to testing.

In the FLIPR assay, HEK-α2β3γ1 cells were tested using the FLIPR® Membrane Potential Assay Kit (Blue), bulk (Molecular Devices, cat #R8034), and Ltk(−)-α2β3γ2 cells were tested using the FLIPR® Membrane Potential Assay Kit (Red), bulk (Molecular Devices, cat # R8123). One vial of each dye was resuspended in 100 mL assay buffer (25 mM HEPES in HBSS pH 7.4) and allowed to fully dissolve. The dye was aliquoted and stored at −20°C until use. The resuspended dye was further diluted by adding 6 to 24 mL of assay buffer (red) and 5.4 to 24.6 mL of assay buffer (blue). All media were carefully aspirated from the induced cells and replaced with 35 μL of either red or blue dye in assay buffer. The cells were incubated for 30 min at 37°C in a humidified atmosphere with 5% CO_2.

The effects of TPA023B and diazepam were evaluated in the presence of a GABA EC_{25} concentration in GABA assay buffer, which contained in mM: 25 HEPES, 10 glucose, 1.25 $CaCl_2$, 1.25 $MgSO_4$, 135 Na^+ gluconate and 5 K^+ gluconate (pH 7.4). Every assay included a 12 point threefold dilution GABA concentration response curve starting at 300 μM for α2β3γ1 and 30 μM for α2β3γ2. TPA023B and diazepam were evaluated at 1 μM GABA for α2β3γ1 and 0.2 μM GABA for α2β3γ2 (the GABA EC_{25} concentrations were determined from separate GABA concentration response curves).

The compounds were first dissolved in DMSO as a 10-mM stock and then further diluted to the testing concentrations so that the final DMSO concentration in the assay was 0.5%. The compounds were screened at 12 concentrations in duplicate from threefold dilutions. The highest concentration was 100 μM in the final assay for TPA023B and 50 μM for diazepam. Five microlitres of the test compound (TPA023B or diazepam) was added to the test well followed by a 10-min incubation before the addition of 10 μL GABA and subsequent incubation for 2 min. Fluorescence was monitored throughout the 15-min protocol. The dyes were excited at wavelength 510–545 nm, and fluorescent signals were recorded at emission wavelength 565–625 nm. The following settings were used: exposure time 0.4 s, data capture 1 read per second, excitation intensity 30% and gain 10%.

The average fluorescence baseline was calculated from the mean of the first 10 readings at the point of GABA addition. All readings were normalised against the average fluorescent baseline. Each time point was then further normalised against the equivalent time data point of the averaged, normalised 'buffer only' sample. The final fluorescence readings after GABA addition were plotted as log [GABA] or log [compound]. EC_{50} values were determined by sigmoidal dose–response curve calculation performed in GraphPad Prism (San Diego, CA, USA). Potentiation by TPA023B relative to diazepam was normalised to the potentiation observed at saturating concentrations of diazepam.

2.11 | Radioligand binding to transiently transfected HEK293 cells

HEK293 cells were grown on 9-cm culture dishes in DMEM medium supplemented with 10% fetal bovine serum and penicillin/streptomycin. Cells were transfected with a total of 8 μg DNA of α2, β3 and γ2 plasmid (ratio: 1:1:3) or α2, β3 and γ1 plasmid (ratio: 1:1:3) using the polyethyleneimine (PEI) method according to the jet-PEI protocol (Polyplus, Illkirch, France, Transfection) and then kept at 37°C and 5% CO_2 for 48 h. For harvesting, culture dishes were washed with ice-cold phosphate-buffered saline (PBS) followed by scraping the cells in buffer and centrifugation at 1000 g for 10 min at 4°C. Cells were resuspended in 20 mM Tris/HCl pH 7.4 containing protease inhibitors (Complete Mini, Roche, Basel Switzerland), homogenised, and centrifuged for 10 min at 1000 g and 4°C. The supernatant was then re-centrifuged for 50 min at 45,000 g and 4°C to obtain the crude membrane fraction. The pellet was resuspended in 20 mM Tris/HCl pH 7.4, 100 mM KCl and stored at −80°C.

For radioligand binding, aliquots of the crude membranes were incubated with increasing concentrations of TPA023B and 2.5 nM [^{3}H]flumazenil (80 Ci mmol^{-1}, ARC) or 1.2 nM of the γ1-selective ligand [^{3}H]γ1sRL (83 Ci mmol^{-1}, custom synthetised by SYNthesis and RcTRI-TEC according to patent WO 2023/213757 A1) in a total volume of 200 μL for 90 min on ice. Subsequently, the samples were filtered onto glass fibre filters using a 12-channnel semi-automated cell harvester (Scatron Instruments AS, Lier, Norway) and washed with ice-cold buffer (20 mM Tris–HCl pH 7.4, 100 mM KCl). Non-specific radioligand binding was determined using equal amounts of membranes prepared from non-transfected HEK293 cells. The radioactivity retained by the filters was determined by liquid scintillation counting using a Tricarb 2500 liquid scintillation analyser. Binding data were analysed using the GraphPad Prism software (version 8.4.3, GraphPad Software, Reston, VA, USA) by a nonlinear one site fit. The K_D values used to calculate the K_i values for TPA023A were 1.0 nM for [^{3}H]flumazenil and 0.56 nM for [^{3}H]γ1sRL.

2.12 | Spinal cord electrophysiology

Transverse 400-μm thick spinal cord slices were prepared from the spinal cord segments L4–L6 of mice 7 days after CCI surgery (for details, see Werynska et al., 2023). Whole-cell patch-clamp recordings were made from superficial dorsal horn neurons of the affected spinal cord side and voltage clamped at −60 mV. Patch pipets were filled with the following internal solution containing (in mM): 120 CsCl, 10 HEPES, 2 $MgCl_2$, 0.05 EGTA, 2 ATP, 0.1 GTP and 5 QX-314. A Cs-based solution was used to block $GABA_B$ receptor-activated K^+ currents. Slices were continuously superfused with the following external solution containing (in mM): 120 NaCl, 2.5 KCl, 26 $NaHC0_3$, 1.25 NaH_2P0_4, 2 $CaCl_2$, 1 $MgCl_2$, 5 HEPES, 15 glucose, continuously gassed with 95% O_2/5% CO_2. An application pipette filled with 1 mM GABA was placed about 500 μm from the recorded neuron. The pipette was connected to a pressure-valve system, and GABA was ejected for 10 ms, every 30 s, for at least 20 min. TPA023B (10 μM) was bath-applied. Data passed the Shapiro–Wilk test for normality and were statistically analysed with a one sample *t*-test.

2.13 | Data and analysis

Studies were designed to generate groups of equal size, and mice were randomly attributed to the different treatment groups. Declared group sizes are the number of independent values, and statistical analyses were performed using these independent values. The different statistical tests applied are detailed in the results section and the figure legends. Statistical significance was assumed for $P < 0.05$. Post-hoc tests were run only if F achieved P<0.05 and there was no significant variance inhomogeneity. All experimenters/data analysts were blinded to the treatment of the mice. Statistical analysis was undertaken for experiments where each group size was at least $n = 5$. When concentration response relationships (Figure 4a,c) and when drug concentrations or receptor occupancy were studied over time (Figures 1c and 3a,f), the number of cells or mice was < 5 for individual time points or concentrations. However, all analyses included all concentrations, such that $n > 5$ for all analyses. For quantification of antihyperalgesia, data were normalised to correct for differences in the degree of sensitisation achieved in individual mice. For quantification of $GABA_AR$ current potentiation, data were also normalised to account for differences in current amplitudes in individual cells. No outliers were excluded. The manuscript complies with the *BJP*'s recommendations and requirements on experimental design and analysis (Curtis et al., 2025). All PK and PK/PD analysis calculations were made using Igor 64 (Wavemetrics; Portland, OR 97223).

2.14 | Nomenclature of targets and ligands

Key protein targets and ligands in this article are hyperlinked to corresponding entries in http://www.guidetopharmacology.org, and are permanently archived in the Concise Guide to PHARMACOLOGY 2023/2024 (Alexander et al., 2023).

3 | RESULTS

3.1 | Antihyperalgesic effect and PKs of TPA023B

We first assessed the antihyperalgesic actions of TPA023B in the chronic constriction injury (CCI) model of neuropathic pain (Figure 1a and Table 1). Following CCI surgery, all mice developed pronounced mechanical hyperalgesia assessed with electronic von Frey filaments. Hyperalgesia was quantified as the reduction in mechanical withdrawal thresholds compared to pre-surgery baselines. Seven to 14 days after CCI surgery, mice were treated orally (p.o.) with three different doses of TPA023B (0.1, 0.3, 1.0 mg kg^{-1}), which elicited

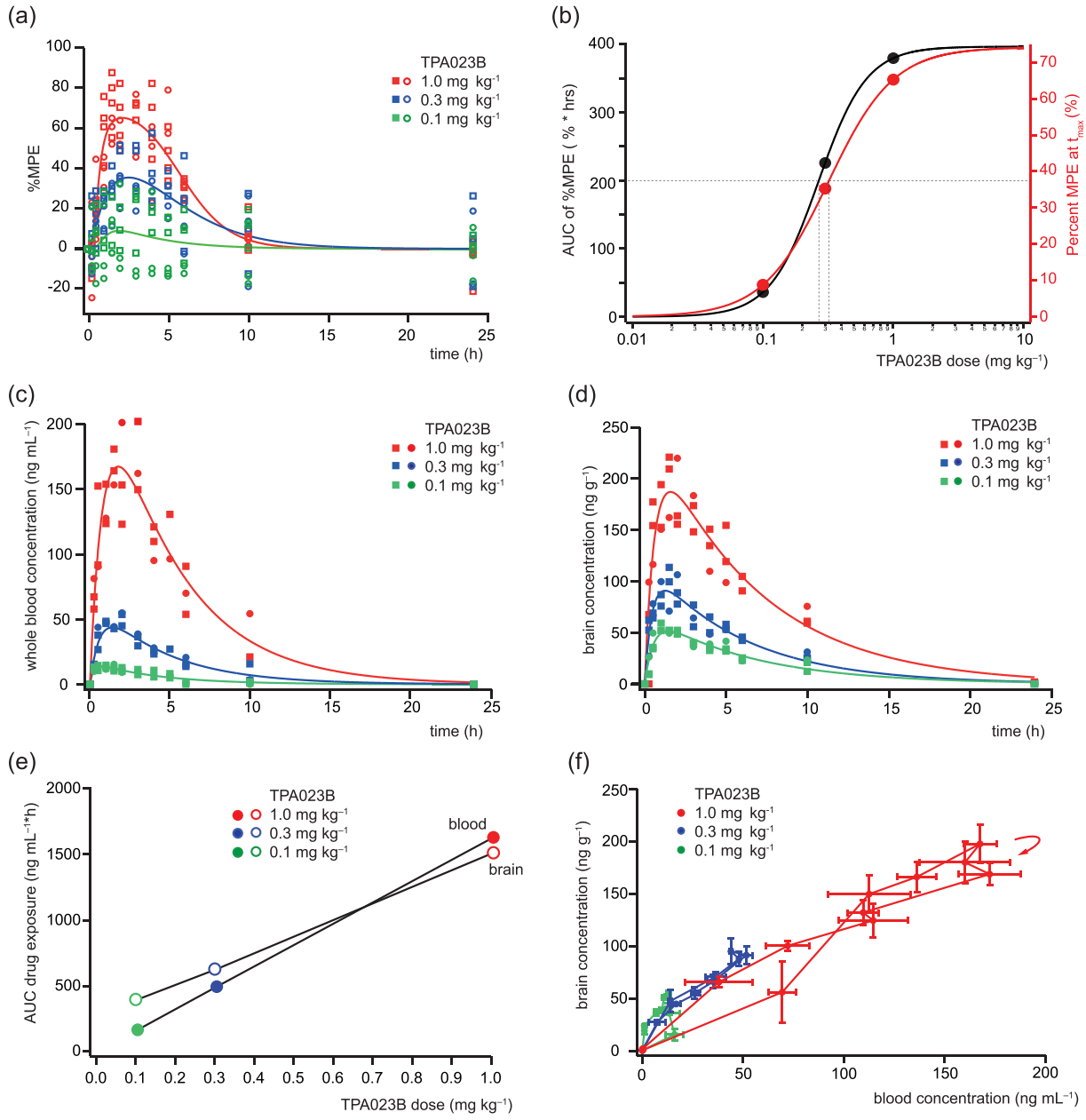

FIGURE 1 Time- and dose-dependent antihyperalgesia by TPA023B, and its pharmacokinetics in whole blood and brain. (a) Dose-dependent antihyperalgesia of TPA023B (0.1, 0.3 and 1.0 mg kg^{-1} body weight). Percent maximum possible effect (MPE) plotted against time. Line, fit of the individual data points to the Bateman function with time-dependent c in the effect compartment (Equations 4 and 5). $n = 6$ mice for 0.1 and 0.3 mg kg^{-1} and $n = 7$ for 10 mg kg^{-1}. (b) Drug effect (AUC of MPE [%MPE·h], black, and Percent MPE at t_{max} (%), red) versus dose. Area under the curve (AUC) values were calculated for each dose from the fitted drug effect from Figure 1a versus time curve integrated over time (0 to 24 h). Solid lines indicate fits to the Hill Equation (7). Dashed lines indicate ED_{50} values. (c) Whole blood concentration of TPA023B (ng mL^{-1}) over time after drug administration. Open symbols, individual mice; closed symbols, mean values. Line, fit of the individual data points to the Bateman function (Equation 3). $n = 3$ mice per dose and time point. (d) Same as Figure 1c but brain tissue concentrations. (e) Drug exposure (AUC of whole blood and brain concentrations plotted over time [0–24 h] Figure 1c and d) versus dose. (f) Brain concentrations (t) plotted versus whole-blood concentrations (t) (mean ± SEM, for both parameters). Red arrow indicates the temporal order of data points obtained with 1 mg kg^{-1} TPA023B.

TABLE 1 Kinetic parameters of antihyperalgesia (values obtained from fits of the data from individual mice to the Bateman function).

dose (mg kg^{-1})	t_{max} (h)	E_{max} (%)	Duration (h)[a]
0.1 ($n = 6$ mice)[b]	1.94	8.96	5.59
0.3 ($n = 6$ mice)	2.78 ± 0.19 (2.59)	31.2 ± 4.6 (35.3)	8.88 ± 0.71 (6.9)
1.0 ($n = 7$ mice)	2.48 ± 0.13 (2.17)	62.8 ± 4.6 (65.3)	7.46 ± 0.34 (6.0)

[a]Time from t_{max} until drug effect declined to less than 20% of its maximum at a given dose.
[b]Because of the small effects of 0.1 mg kg^{-1}, it was not possible to calculate t_{max}, E_{max} and duration for individual mice. Therefore, only an average value is reported derived from the fit of the %MPE values of the three 6–7 mice tested per dose plotted versus time.

TABLE 2 Pharmacokinetic parameters of TPA023B in whole blood and brain ($n = 3$ mice)[a].

	t_{max}		c_{max}		Terminal half-life ($t_{1/2}$)[b]	
dose (mg kg^{-1})	blood (h)	Brain (h)	Blood (ng mL^{-1})	Brain (ng g^{-1})	blood (h)	brain (h)
0.1	0.56 ± 0.16 (0.72)	1.45 ± 0.14 (1.46)	15.5 ± 1.25 (14.0)	51.5 ± 0.3 (51.4)	2.77 ± 0.18 (3.1)	4.40 ± 0.73 (4.38)
0.3	1.61 ± 0.08 (1.39)	1.21 ± 0.14 (1.25)	52.2 ± 1.91 (44.0)	91.2 ± 1.7 (91.2)	2.28 ± 0.84 (3.0)	4.02 ± 0.33 (4.05)
1.0	1.77 ± 0.21 (1.75)	1.61 ± 0.08 (1.58)	169 ± 1.84 (168.7)	188 ± 6.0 (188)	3.01 ± 0.74 (3.1)	4.43 ± 0.10 (4.50)

[a]Values in brackets are derived from the fit of all the c_{blood} or c_{brain} values obtained from the three mice tested per dose plotted versus time.
[b]$t_{1/2}$ was calculated from the rate constant of elimination (k_e).

dose- and time-dependent antihyperalgesia. Maximal antihyperalgesia obtained with 1 mg kg^{-1} TPA023B was about 60–65% reduction in mechanical hyperalgesia. It was reached between 2.5 and 2.8 h after drug administration. To estimate the dose required to achieve the half-maximal anti-allodynic effect, we plotted the percent MPE at t_{max} and the AUC of curves shown in Figure 1a versus the applied dose. Fits to the Hill equation (7) show that the half maximal effective dose (ED_{50}) was 0.32 and 0.27 mg kg^{-1} for the two analyses, respectively (Figure 1b). From that analysis, we estimate that saturating doses of TPA023B will reduce hyperalgesia by 75% at t_{max}.

PK properties of TPA023B after oral administration were characterised in whole blood and brain (Figure 1c,d and Table 2). Whole blood and brain concentrations were measured in separate groups of three mice each at the same time points at which the antihyperalgesic activity of TPA023B had been measured. Again, single oral doses of 0.1, 0.3 and 1.0 mg kg^{-1} were administered. Average maximum whole blood concentrations determined from fits to the Bateman function (Equation 3) were 15.5, 52.2 and 169 ng mL^{-1} for 0.1, 0.3 and 1.0 mg kg^{-1} TPA023B, respectively, and terminal half-lives, also determined from fits to the Bateman function, were between 2.28 and 3.01 h.

Average maximum brain concentrations were 51.2, 91.2 and 188 ng mL^{-1} for 0.1, 0.3 and 1.0 mg kg^{-1} TPA023B, respectively, and half-life varied between 4.02 and 4.43 h (Figure 1d and Table 2). Assuming that 0.73 ± 0.03% (determined in rat brain tissue; unpublished data) of the total drug being unbound, these values yield free drug concentrations of 0.96 ± 0.04, 1.70 ± 0.07 and 3.50 ± 0.14 nM. The time points at which maximal drug concentrations were reached (t_{max}) were similar for whole blood and brain (between 0.56 and 1.77 h and between 1.21 and 1.61 h, for whole blood and brain, respectively). Drug exposure area under the curve (AUC) increased linearly with dose for both whole blood and brain (Figure 1e).

To determine to what extent TPA023B penetrates across the blood brain barrier, we plotted for each time point brain concentrations versus whole blood concentrations (Figure 1f). Our results show a good correlation of whole blood and brain levels. Ratios of brain versus whole-blood exposure (AUCs) decreased slightly with increasing doses (2.37, 1.27 and 0.93, for 0.1, 0.3 and 1.0 mg kg^{-1}). Our results also indicate that brain concentrations followed whole blood concentrations with no obvious delay, as indicated by the absence of counterclockwise hysteresis in the brain versus whole blood concentrations (Figure 1f). These results confirm a quick penetration of TPA023B through the blood brain barrier.

3.2 | Pharmacokinetic/pharmacodynamic (PK/PD) properties of TPA023B

Comparing the time courses of TPA023B-induced antihyperalgesia and TPA023B concentration in the brain (Figures 1a and d) shows that antihyperalgesia by TPA023B declined faster than its brain concentrations, hinting at possible tolerance development. Tolerance against the sedative effects of several classical non-selective BDZ site agonists has been repeatedly reported manifesting in clockwise hysteresis in human PK/PD studies (Barbanoj et al., 2007; Ellinwood et al., 1984; Luurila & Olkkola, 1996; Wright et al., 1997). We therefore plotted TPA023B-induced antihyperalgesia against the whole blood concentration of TPA023B for all time points, at which drug concentrations and antihyperalgesic effects had been determined (Figure 2a). For all three doses (0.1, 0.3 and 1.0 mg kg^{-1}), a given drug concentration produced stronger antihyperalgesia during the falling phase of drug concentrations than when drug concentrations were rising, demonstrating counterclockwise rather than clockwise hysteresis and arguing against tolerance development.

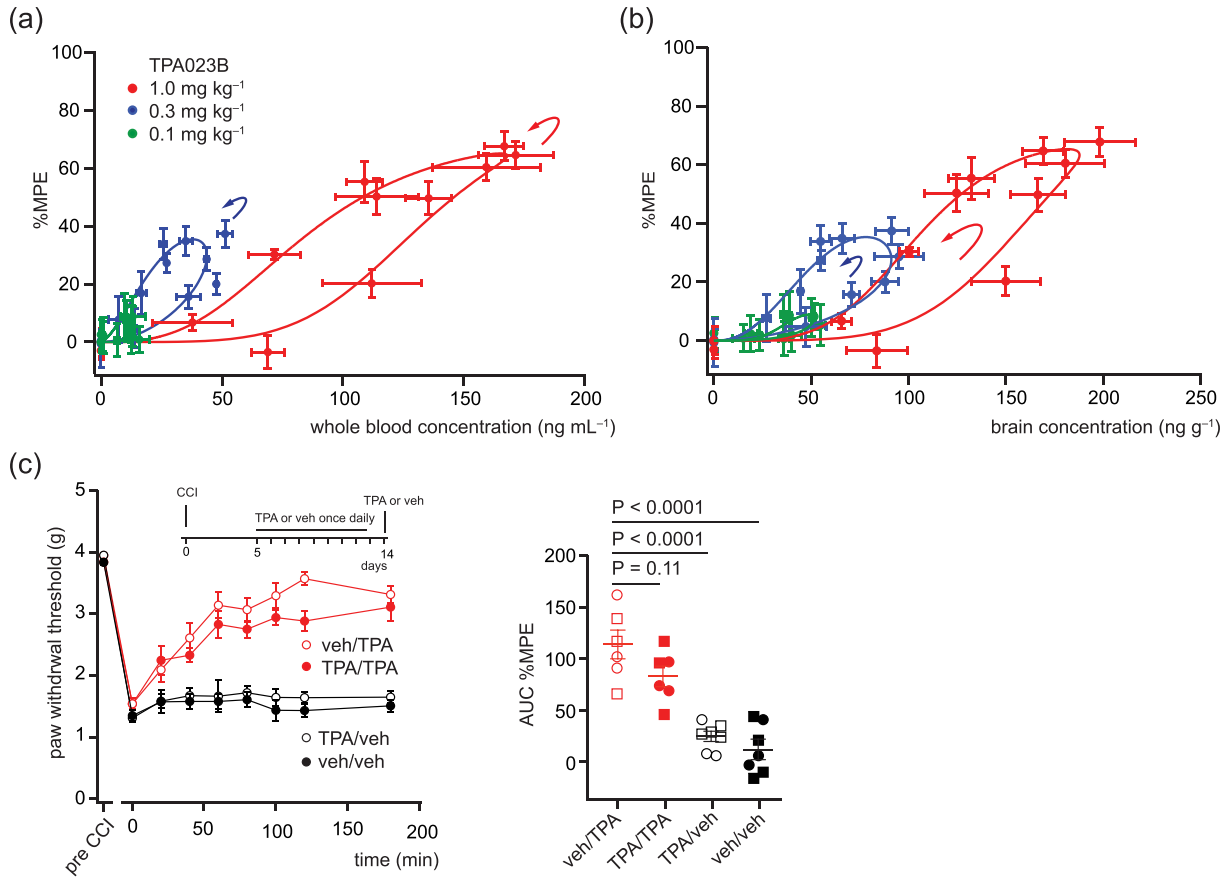

FIGURE 2 Pharmacokinetic/pharmacodynamic (PK/PD) modelling. (a) Percent maximum possible effect (MPE) antihyperalgesia (%MPE(t)) plotted versus whole-blood drug concentrations ($c_{blood}(t)$). Mean ± SEM, for both parameters. Curves show fits of effect data to the Hill Equation (4) with time-dependent drug concentrations (Equation 5) plotted versus the fits for $c_{blood}(t)$ to the Bateman function (Equation 3). Arrows indicate temporal order of data points (counterclockwise hysteresis). Number of mice $n = 6$ or 7 für %MPE, $n = 3$ for concentrations measurements see also figure legend 1. (b) Same as Figure 2a but for brain concentrations. (c) Efficacy of TPA023B after a 9-day once-daily treatment. veh/TPA, mice pretreated with veh (vehicle) and tested with TPA023B on day 10; veh/veh, mice pretreated with veh and tested with veh; TPA/TPA, mice pretreated with TPA023B and tested with TPA023B; TPA/veh, mice pretreated with TPA023B and tested with veh. $n = 6$ mice for veh/TPA and TPA/TPA, $n = 7$ mice for veh/veh and TPA/veh. Left: time course of anti-allodynia following treatment with TPA023B or vehicle. Inset illustrates experimental design. Significant differences in the degree of anti-hyperalgesia were found between baseline (time 0) and all subsequent time points ≥ 40 min and ≥ 60 min for TPA/TPA (repeated measures one-way ANOVA followed by Dunnett's multiple comparisons test; $F[5,35] = 8.31$) and veh/TPA ($F[5,35] = 2.04$), respectively. No significant differences were found between TPA/TPA and veh/TPA for any of the time points (one-way ANOVA $F[15,80] = 11.69$ Sidac's post hoc test). Right: AUC of antihyperalgesia (0–120 min). Circles, female mice; squares, male mice. One-way ANOVA followed by Dunnett's multiple comparison test with veh/TPA single dose treatment as reference, $F(3,22) = 24.2$.

Delayed drug exposure of the putative effect compartment relative to the compartment in which drug concentrations were measured is a frequent cause of counterclockwise hysteresis. Because previous work has shown that the antihyperalgesic effect of subtype-selective BDZ site agonists originates from the CNS, we repeated these analyses with brain instead of whole blood concentrations (Figure 2b). These analyses yielded very similar counterclockwise hysteresis for all three doses, ruling out delayed penetration into the brain as a cause underlying the counterclockwise hysteresis.

The counterclockwise hysteresis found for both whole blood and brain concentrations strongly argue against acute tolerance development. To complement these experiments, we tested whether a chronic 9-day long once-daily pretreatment with 1 mg kg^{-1} TPA023B would induce tolerance. Previous experiments from our group with a non-selective BDZ site agonist (diazepam) had revealed pronounced tolerance development in the same dosing regimen (Ralvenius et al., 2015). Antihyperalgesic actions of TP023B measured in TPA023B pretreated mice were only slightly smaller than in naïve mice (AUC [%MPE·time] = 112.7 ± 14.0%·h versus 83.2 ± 10.3%·h, $P = 0.11$, in pretreated versus drug naïve [vehicle treated] mice, respectively) (Figure 2c).

3.3 | Receptor occupancy by TPA023B in brain and spinal cord

$GABA_AR$ occupancy was measured using a tritiated version of the BDZ site antagonist flumazenil ([^{3}H]flumazenil) as the radioligand

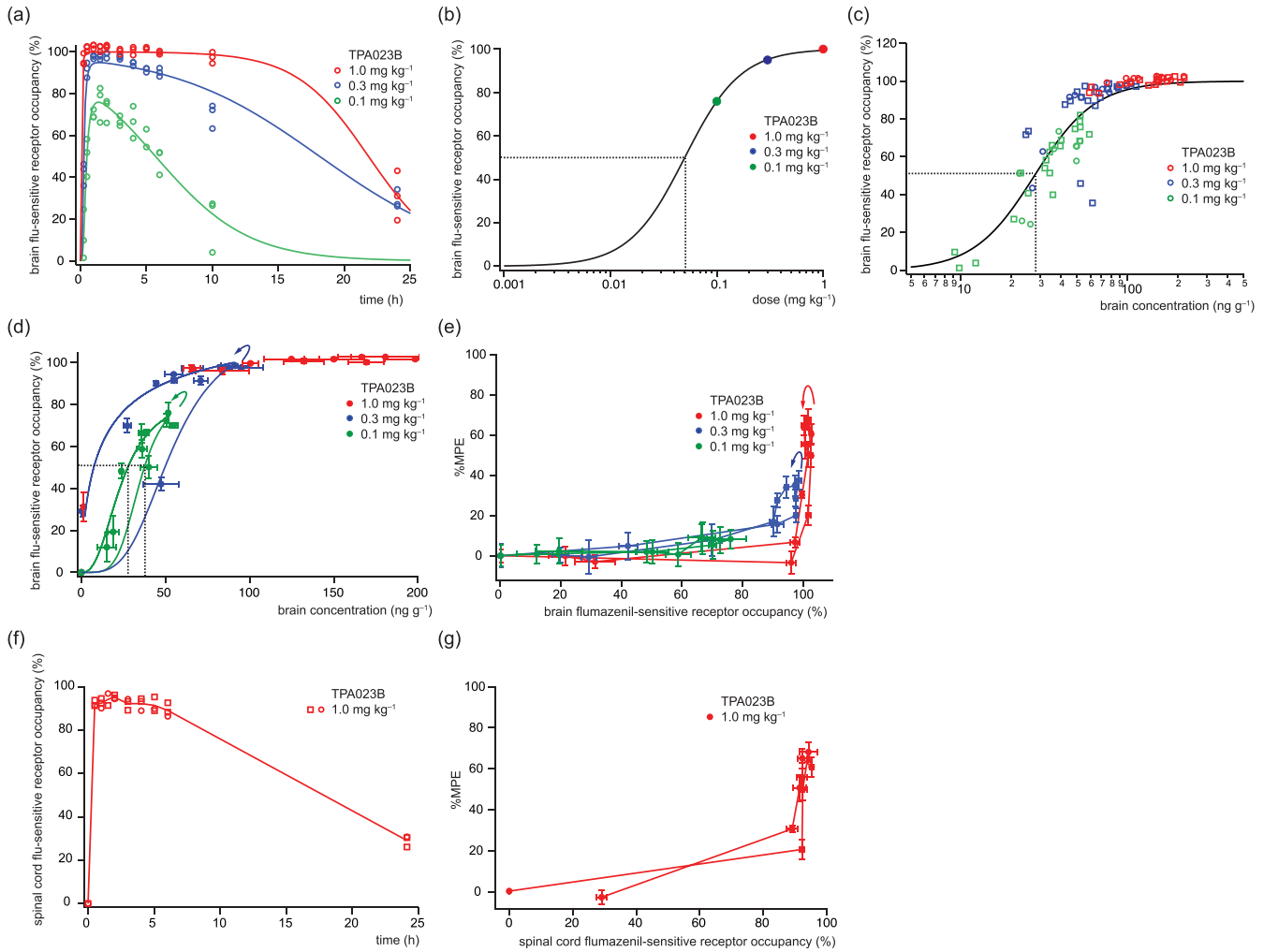

FIGURE 3 TPA023B exposure of brain and spinal cord. (a) Flumazenil-sensitive receptor occupancy (RO) by TPA023B in brain (RO(*t*)) versus time after drug administration (*t*). Symbols represent individual mice. Line, fit of the individual data points to the Hill Equation (8) with time-dependent drug concentrations in the hypothetical effect compartment (Equation 9). $n = 2$ or 3 mice per time point and dose. (b) Dose dependence of RO. Data points are maximal RO values obtained from Figure 3a. Line, fit to the Hill equation (Equation 10). Dotted line illustrates ED_{50}. (c) RO plotted versus c_{brain}. Symbols indicate individual mice. Colours indicate the different doses. Solid line, fit to the Hill equation (Equation 11). Dotted line illustrates EC_{50}. Number of mice $n = 36$ per dose. (d) Time dependent flumazenil-sensitive RO in brain (RO($c(t)$)) plotted versus c_{brain} (*t*). Mean ± SEM for both parameters. Curves show fits of RO values to the Hill equation (Equation 8) with time-dependent whole-blood drug concentrations (Equation 9) plotted versus the fits for $c_{blood}(t)$ to the Bateman function (Equation 3). Arrows indicate temporal order of data points (counterclockwise hysteresis). Number of mice $n = 3$ per time point and dose. (e) Time-dependent maximum possible antihyperalgesia (percent MPE (RO(*t*)) plotted versus RO(*t*)). Mean ± SEM for both parameters. Arrows indicate temporal order of data points (counterclockwise hysteresis). Number of mice $n = 6$ or 7 (for %MPE) and $n = 2$ or 3 (for receptor occupancy) per time point and dose. (f, g) Same as Figures 3a and e, but spinal cord. Only the dose of 1.0 mg kg^{-1} was tested. $n = 3$ mice per dose for RO measurements. $n = 2$ or 3 mice per time point (f), $n =$ 6 or 7 mice per data point (g).

(Figure 3). TPA023B produced a dose- and time-dependent occupancy of brain $GABA_A$Rs with maximum levels reached between 1.4 and 0.9 h after TPA023B administration. Maximum RO were 75.9%, 94.9% and 99.9% for 0.1, 0.3 and 1.0 mg kg^{-1} TPA023B, respectively (Figure 3a and Table 3). Fitting the data to the Hill equation (Equation 10) yielded a dose of 0.05 mg kg^{-1} required for 50% RO (Figure 3b). Although this value is in good agreement with previous data (Atack et al., 2011), it has been derived from only three data points which all fall into the RO range above 75%. Plots of RO versus brain concentrations allowed us to estimate the *in vivo* affinity of TPA023B at mouse brain $GABA_A$Rs. Fitting the data to the Hill equation yielded a brain concentration inducing 50% RO of 27.7 ± 1.3 ng g^{-1}, equivalent to an affinity of 71 ± 3.3 nM (Figure 3c).

TABLE 3 Kinetics of receptor occupancy ($n = 3$ mice).

Dose (mg kg^{-1})	t_{max} (*h*)	RO_{max} (%)
0.1	1.38	75.9 ± 5.01
0.3	1.38	94.9 ± 0.82
1.0	n.d.	99.9 ± 0.32

Subsequently, we plotted for all measured time points RO (RO(*t*)) over brain concentration ($c_{brain}(t)$) to gain additional insights into possible processes underlying the counterclockwise hysteresis in the *E*(*t*) versus *c*(*t*) plots (Figure 3d). Unexpectedly, this analysis revealed again a counterclockwise hysteresis this time in the RO(*t*) over $C_{brain}(t)$ plot. Such a behaviour is typically seen with drugs that show very slow unbinding from the receptor (Louizos et al., 2014). This explanation is supported by the still 30–40% RO found at 24 h after drug administration when brain concentrations were already below the quantification limit (compare Figure 1d).

We finally used the RO data to also investigate how TPA023B-induced antihyperalgesia correlates with brain RO. We plotted brain RO(*t*) versus the percent maximum possible antihyperalgesia *E*(*t*) (Figure 3e). This analysis indicated that an almost complete RO (> 90%) was needed to achieve significant (> 20%) antihyperalgesia. Moreover, especially with the highest dose of TPA023B (1 mg kg^{-1}), antihyperalgesic effects continued to increase over time even though RO was already virtually complete. We considered that the spinal cord rather than the brain is the primary site of the antihyperalgesic action of TPA023B (Paul et al., 2014) and that TPA023B kinetics in spinal cord might differ from those in the brain. We therefore repeated the RO measurements for the highest dose of TPA023B in spinal cord tissue (Figure 3f,g). These analyses yielded results very similar to those obtained for the brain, ruling out major differences in RO between brain and spinal cord.

The data thus suggest that antihyperalgesia by TPA023B was not evoked by the receptor population whose occupancy was detected with [^{3}H]flumazenil. Yet, previous findings by our group had indicated that the sensory effects of TPA023B occur exclusively through $GABA_A$Rs (Ralvenius et al., 2018). Collectively, these results suggest an involvement of $GABA_A$Rs that are not detected with [^{3}H]flumazenil. In fact, flumazenil binds γ2 and γ3 $GABA_A$R with much higher affinity than γ1 $GABA_A$R, opening the possibility that TPA023B exerted its antihyperalgesic activity mainly via γ1 $GABA_A$Rs. In line with this, recent work from our group has shown that besides γ2 $GABA_A$Rs, γ1 $GABA_A$Rs are densely expressed in the spinal dorsal horn (Neumann et al., 2024). We therefore tested whether TPA023B modulates not only γ2- but also γ1-$GABA_A$Rs.

3.4 | γ $GABA_A$R subtype selectivity of TPA023B

We analysed the binding and modulatory effects of TPA023B on recombinant γ2- and γ1- $GABA_A$Rs transiently expressed in HEK293 cells (Figure 4). Because most of the antihyperalgesic effect of $GABA_A$R PAMs occurs through α2-$GABA_A$Rs (Knabl et al., 2008; Ralvenius et al., 2015), we tested TPA023B on recombinant $GABA_A$Rs containing an α2 subunit in combination with β3 and either γ1 or γ2 subunits. In competition radioligand binding assays, TPA023B inhibited with high potency [^{3}H]flumazenil binding to α2β3γ2 receptors (K_i value: 4.7 ± 1.5 nM) and with lower affinity [^{3}H]γ1sRL binding to α2β3γ1 receptors (K_i value: 599 ± 188 nM) (Figure 4a), demonstrating that TPA023B also binds to α2β3γ1 $GABA_A$Rs. In a functional assay,

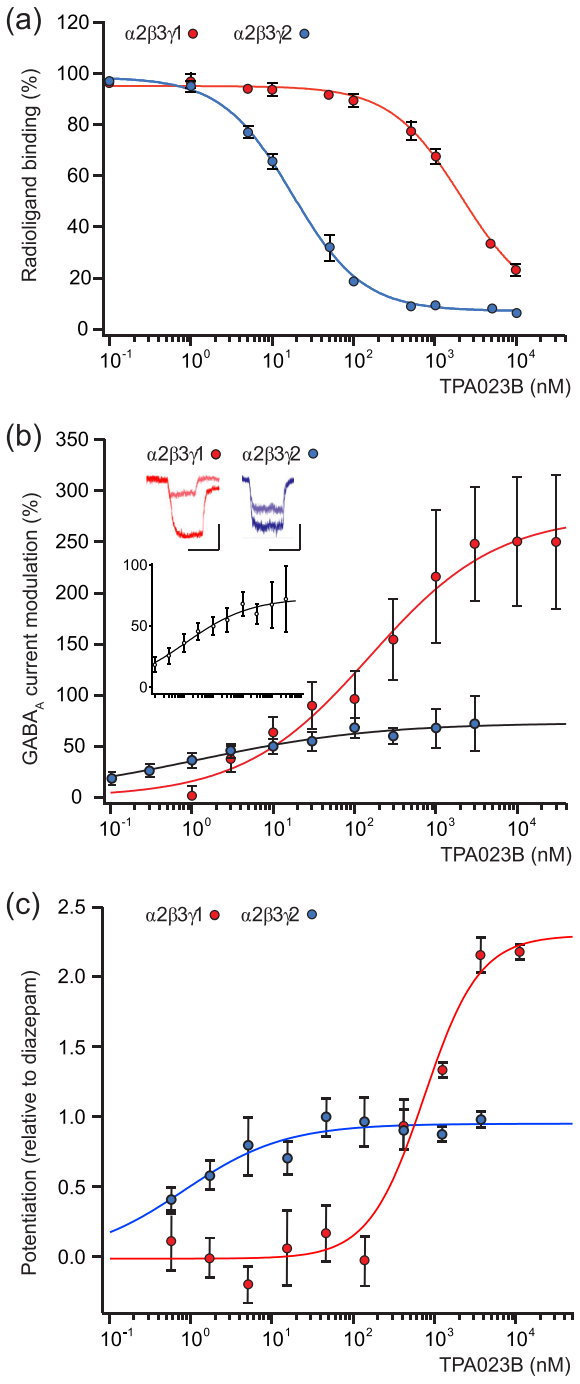

FIGURE 4 Legend on next page.

TPA023B, as expected, increased the amplitudes of GABA evoked currents through α2β3γ2 (Figure 4b). This effect occurred with an EC_{50} of 0.95 ± 0.35 nM. Maximum potentiation estimated from a fit of the data to the Hill equation was 73.0 ± 3.7%. These values are in good agreement with previous data (Atack et al., 2011). We also observed a pronounced potentiation of $GABA_A$R currents through α2β3γ1-$GABA_A$Rs with lower potency but with much higher efficacy. Fits to the Hill equation yielded an EC_{50} value of 153 ± 51 nM and an E_{max} of 276 ± 20%. The potency of TPA023B in the electrophysiology

assay was confirmed in studies using a fluorescence-based assay that detects the change in membrane potential. In this orthogonal indirect measure of $GABA_AR$ function, TPA023B had a PAM activity of around 1 and 500 nM in cells expressing α2β3γ2- and α2β3γ1-$GABA_ARs$, respectively. Figure 4c shows the data relative to diazepam to normalise between different cell types and different assay membrane potential dye. The latter two assays demonstrate that TPA023B not only potentiates γ2- but also γ1-$GABA_ARs$ and that potentiation of γ1-$GABA_ARs$ occurs with an about 100-fold to 500-fold lower potency.

FIGURE 4 Binding of TPA023B to γ1 and γ2 G $GABA_A$receptors and potentiation by TPA023B. (a) Binding of TPA023B to α2β3γ1 and α2β3γ2 $GABA_ARs$. Mean ± SD of 5 ([^{3}H]flumazenil binding) and 3 ([^{3}H]γ1sRL binding) independent experiments. Affinities of [^{3}H] flumazenil to α2β3γ2 $GABA_ARs$ and of [^{3}H]γ1sRL to α2β3γ1 $GABA_ARs$ are similar (0.56 nM [Benke et al., 1994] and 1.0 nM [Graham et al., 1996]). (b) Concentration–response curves for the potentiating action of TPA023B on GABA evoked currents through α2β3γ1 and α2β3γ2 $GABA_ARs$. Mean ± SEM. Solid lines are fits to the Hill equation. $n = 9–11$ cells per concentration for α2β3γ1, and 9–20 cells per concentration for α2β3γ2. Insets show example traces before (light colour) and during the application of TPA023B (3 μM) (dark colour). Scale bars, 100 pA, 2 s, for α2β3γ1; 200 pA, 2 s, for α2β3γ2. (c) Concentration–response curves from Fluorometric imaging plate reader (FLIPR) assay for the modulation of TPA023B relative to diazepam in HEK-α2β3γ1 and Ltk-α2β3γ2 at GABA EC_{25}, with $EC_{50} \sim 500$ nM and ~1 nM respectively. Mean ± SEM. Nonlinear regression log (agonist) versus response variable slope. $n = 4$ wells per concentration with $n = 3$ replicates. Note that the data for α2β3γ1 and α2β3γ2 were obtained with different fluorescent indicators and different cells types; therefore, the data are expressed relative to diazepam. Maximal fluorescence values cannot be compared between the two receptor subtypes.

3.5 | Potentiation of $GABA_AR$ currents in dorsal horn neurons of mice with peripheral nerve injury

We have previously shown that non-selective (diazepam; Knabl et al., 2008) and subtype-selective (TPA023B; Ralvenius et al., 2018) BDZ site agonists potentiate $GABA_AR$ currents in dorsal horn neurons of healthy mice. To better link these cellular effects to the antihyperalgesic actions of TPA023B in nerve injured mice, we tested if TPA023B would potentiate $GABA_AR$ currents in superficial dorsal horn neurons of nerve injured mice (Figure 5). In the absence of TPA023B, GABA evoked membrane currents with average amplitudes of 72.9 ± 29.6 pA ($n = 5$). Application of TPA023B (10 μM) potentiated these currents on average by 34 ± 12% ($P < 0.05$, one sample t-test). These results confirm previous behavioural studies (Neumann et al., 2021; Paul et al., 2014) and further support that TPA023B exerts its antihyperalgesic actions through a potentiation of GABAergic inhibition in the spinal dorsal horn.

4 | DISCUSSION

4.1 | Pharmacokinetic (PK) characteristics of TPA023B in mice

PK characteristics of TPA023B have been reported previously for various species including mouse, rat, dog and man (Atack, 2009; Atack et al., 2011). In vitro affinity of TPA023B measured in this study for human $GABA_ARs$ expressed in HEK293 cells (4.7 nM) was similar to those determined previously for the same human recombinant receptors (2 nM; Atack et al., 2011) and for rat native receptors (0.99 nM; Atack et al., 2011). This value is about 15-times lower than the apparent in vivo affinity determined in the present study (28 ng g^{-1} or

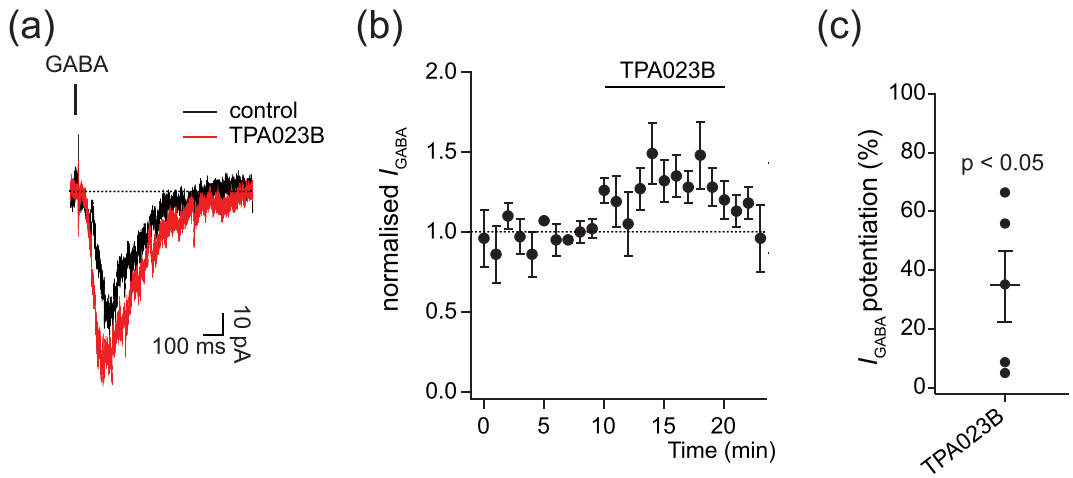

FIGURE 5 Potentiating effects of TPA023B on $GABA_AR$ currents in superficial dorsal horn neurons of neuropathic mice. (a) Example traces of $GABA_A$receptor evoked membrane currents recorded before and during the application of TPA023B (10 μM) in transverse lumbar spinal cord slices prepared from mice 7 days after CCI surgery. (b) Time course (mean ± SEM) of normalised $GABA_AR$ current amplitudes in $n = 5$ neurons prepared from five mice. (c) Potentiation of $GABA_AR$ currents. Amplitude ratios (averages of the last five traces recorded in the presence of TPA023B versus control conditions) were significantly different from unity ($P < 0.05$, one sample t-test, $n = 5$ neurons).

71 nM total brain concentration). This difference is likely because of the small fraction of the total brain TPA023B that is free (0.73%, unpublished data). Previous studies and our study report similar oral TPA023B doses required to reach 50% RO in mice (0.11 and 0.05 mg kg^{-1}). Previous work has found large differences in the PK properties of TPA023B between species (human, dog and rat), with a much shorter half-life and t_{max} in dogs compared to rat and human (Atack, 2009). The values reported there for dogs are similar to those reported here for mice.

4.2 | Tolerance development

Many effects of classical non-selective BDZ site agonists such as sedation and anxiolysis undergo pronounced PD tolerance. Acute tolerance occurring during drug exposure following a single dose manifests in PK/PD studies as clockwise hysteresis when time-dependent drug effects ($E(c(t))$ are plotted against time-dependent drug concentrations ($c(t)$). The underlying mechanisms are still unknown, but in case of tolerance development to the antihyperalgesic effects, an intracellular accumulation of chloride has recently been proposed (Lorenzo et al., 2020).

Clockwise hysteresis was not detected in our study, and we rather found counterclockwise hysteresis both for plots of effect versus whole-blood or brain concentrations, suggesting that no tolerance had developed. Accordingly, chronic (9-day) treatment experiments revealed a relatively small and statistically insignificant loss of efficacy in mice pretreated with TPA023B relative to naïve (vehicle pretreated) mice. Previous work from our group has shown that antihyperalgesia induced with the non-selective BDZ site agonist diazepam is subject to tolerance development (Ralvenius et al., 2015). Clockwise hysteresis was also observed for the antihyperalgesic activity of N-desmethyl clobazam, a BDZ site ligand with reduced sedative properties (Besson et al., 2013; Ralvenius et al., 2016). Other previous experiments from our group (Ralvenius et al., 2015) and from others (van Rijnsoever et al., 2004) have suggested that the subtype selectivity of BDZ site ligands is a major determinant of tolerance liability. The present experiments with TPA023B further support that $GABA_AR$ subtype selectivity is a major determining factor.

Typical explanations of counterclockwise hysteresis include delayed penetration of the drug into the effect compartment or the generation of active metabolites (Louizos et al., 2014). In our experiments, counterclockwise hysteresis was not only seen in the plots against whole-blood concentrations but also when antihyperalgesic activity was plotted against brain concentrations, ruling out delayed penetration into the brain as an underlying mechanism. t_{max} was in fact nearly identical for whole-blood and brain concentrations. An alternative explanation is the generation of an active metabolite. However, previous work found no TPA023B metabolites in the brain (Atack et al., 2011). Sensitisation or up-regulation of receptors can also lead to counterclockwise hysteresis. Interestingly, spinal α2- and α3- $GABA_ARs$ have been reported to be up-regulated following peripheral nerve injury (Lorenzo et al., 2020). However, this process is likely too slow to account for the hysteresis seen here. Other results of the present study hint at different explanations. We not only observed counterclockwise hysteresis for the antihyperalgesic action of TPA023B but also when RO, instead of antihyperalgesia, was plotted against brain concentrations (Figure 3d). This latter hysteresis is most likely explained by a very low rate of the unbinding of TPA023B from $GABA_ARs$ (see also Louizos et al., 2014). Additionally, even more downstream mechanisms may also contribute. Plots of drug effect versus RO also showed some counterclockwise hysteresis, suggesting a certain delay between receptor binding and the antihyperalgesic action. Such delays can be caused by a progressive series of molecular events (Campbell, 1990; Louizos et al., 2014) required to reduce hyperalgesia following the binding of TPA023B to its receptors. Such molecular events might include signalling steps reverting pronociceptive neuroplastic changes by enhanced inhibition in nociceptive circuits.

4.3 | Possible involvement of γ1 $GABA_ARs$

A very unexpected finding of our study was made when we plotted the magnitude of TPA023B-induced antihyperalgesia versus RO. We found that the antihyperalgesic effect increased steeply over time only when RO was already almost complete, supposedly disconnecting the antihyperalgesic effect from $GABA_AR$ RO and suggesting that TPA023B acted through receptors that were not detected with the radioligand [^{3}H]flumazenil. These could in principle include receptors not belonging to the $GABA_AR$ family. We have, however, previously shown that TPA023B acts exclusively through $GABA_ARs$ (Ralvenius et al., 2018). Important in this context is that flumazenil exhibits high affinity binding only at γ2 (and to a lesser extent γ3) $GABA_ARs$, while it has negligible affinity at γ1-$GABA_ARs$ (Wingrove et al., 1997). Interestingly, the spinal dorsal horn, which is the main site of the antihyperalgesic action of subtype-selective $GABA_AR$ PAMs (Paul et al., 2014), expresses besides γ2- $GABA_ARs$ also γ1- $GABA_ARs$, while it virtually lacks γ3-$GABA_ARs$ (Neumann et al., 2024). Electrophysiological experiments in the present study showed that TPA023B not only potentiates γ2-$GABA_ARs$, but with lower potency yet even higher efficacy also γ1- $GABA_ARs$, rendering possible that γ1-$GABA_ARs$ make a significant contribution to the antihyperalgesic effect of TPA023B, while flumazenil detected RO at γ2- $GABA_ARs$. Given the relatively low abundance of γ1 $GABA_ARs$ (relative to γ2 $GABA_ARs$) and the relatively low RO of γ1 $GABA_ARs$ expected at TPA023B concentrations reached in vivo in this study, one might question the potential contribution of γ1 $GABA_ARs$. However, γ1 $GABA_ARs$ may be enriched in certain subpopulation of dorsal horn neurons or may have specific subcellular localisations, for example, on axon terminals or axon initial segments, where a relatively low number of receptors may have strong effects on excitability or synaptic transmission.

Besides TPA023B, several non-selective or α2/α3-$GABA_AR$ subtype selective BDZ site agonists exhibit antihyperalgesic activity in

rodent or human pain models. These include diazepam (Knabl et al., 2008; Knabl et al., 2009), midazolam (Ralvenius et al., 2015), L-838′417 (Knabl et al., 2008; Lorenzo et al., 2020; Nickolls et al., 2011; Reichl et al., 2012), HZ-166 (Di Lio et al., 2011), KRM-II-081 (Lewter et al., 2024), NS16085 (Lewter et al., 2024), PF-0637286 (van Amerongen et al., 2019) and N-desmethyl clobazam (Besson et al., 2013; Di Lio et al., 2011). All these compounds bind and modulate γ2-$GABA_A$Rs. So far, only three of them—diazepam (Khom et al., 2006), midazolam (Khom et al., 2006) and HZ-166 (Neumann et al., 2024)—have been reported to also exhibit activity at γ1-$GABA_A$Rs, whereas for the others, no such information is currently available. It will be informative to determine the extent to which activity at γ1-$GABA_A$Rs correlates with antihyperalgesic efficacy.

Several previous studies have found that antihyperalgesic effects of BDZ site agonists can be attenuated by flumazenil to variable degrees (Di Lio et al., 2011; Knabl et al., 2008; Lewter et al., 2017; Lewter et al., 2024), indicating that part of the antihyperalgesia originated with γ2-$GABA_A$Rs. The relative contribution of γ1-$GABA_A$Rs versus γ2-$GABA_A$Rs will probably vary between compounds depending on their relative potency and efficacy at the two receptor subtypes.

4.4 | Implications

In summary, the TPA023B PK/PD relationship for antihyperalgesia could not be simply accounted for by occupancy of γ2-$GABA_A$Rs. Together with the electrophysiology experiments, these results therefore provide further support for an involvement of γ1- $GABA_A$Rs in spinal nociceptive processing and suggest γ1-$GABA_A$Rs as potential targets for novel analgesics. TPA023B is, in fact, well tolerated in mice (Ralvenius et al., 2018) and in humans (Atack et al., 2011), and the apparent absence of tolerance liability may further support its clinical usefulness.

AUTHOR CONTRIBUTIONS

Elena Neumann: Funding acquisition (equal); investigation (equal); methodology (equal); writing—original draft (equal); writing—review and editing (equal). **Mariana O. Popa:** Methodology (equal); supervision (lead); writing—review and editing (equal). **Karen T. Elvers:** Investigation (equal); methodology (equal); resources (equal); visualization (equal); writing—review and editing (equal). **Misa Oyama:** Data curation (equal); formal analysis (equal); investigation (equal); methodology (equal); visualization (equal); writing—review and editing (equal). **Daniel Ulrich:** Formal analysis (equal); investigation (equal); methodology (equal); visualization (equal); writing—review and editing (equal). **Marcus Hanley:** Investigation (equal); methodology (equal). **Gui Jie Feng:** Investigation (equal); methodology (equal); writing—review and editing (equal). **Thomas Hathaway:** Investigation (equal); writing—review and editing (equal). **William T. Ralvenius:** Conceptualization (equal); methodology (equal); writing—review and editing (equal). **Thomas Grampp:** Investigation (equal); methodology (equal). **Dietmar Benke:** Formal analysis (equal); investigation (equal); methodology (equal); resources (equal); visualization (equal); writing—review and editing (equal). **John R. Atack:** Conceptualization (equal); data curation (equal); funding acquisition (equal); supervision (equal); writing—review and editing (equal). **Hanns Ulrich Zeilhofer:** Conceptualization (lead); formal analysis (lead); funding acquisition (equal); software (lead); supervision (lead); writing—original draft (lead); writing—review and editing (lead).

ACKNOWLEDGEMENTS

The authors thank Louis Scheurer and Thomas Grampp for excellent technical assistance. Open access publishing facilitated by Universitat Zurich, as part of the Wiley - Universitat Zurich agreement via the Consortium Of Swiss Academic Libraries.

CONFLICT OF INTEREST STATEMENT

The authors declare no conflict of interest.

DATA AVAILABILITY STATEMENT

The data that support the findings of this study are openly available in Zenodo at https://doi.org/10.5281/zenodo.15560921.

DECLARATION OF TRANSPARENCY AND SCIENTIFIC RIGOUR

This Declaration acknowledges that this paper adheres to the principles for transparent reporting and scientific rigour of preclinical research as stated in the *BJP* guidelines for Design and Analysis, and Animal Experimentation, and as recommended by funding agencies, publishers and other organisations engaged with supporting research.

ORCID

Hanns Ulrich Zeilhofer https://orcid.org/0000-0001-6954-4629

REFERENCES

Alexander, S. P. H., Mathie, A. A., Peters, J. A., Veale, E. L., Striessnig, J., Kelly, E., Armstrong, J. F., Faccenda, E., Harding, S. D., Davies, J. A., Aldrich, R. W., Attali, B., Baggetta, A. M., Becirovic, E., Biel, M., Bill, R. M., Caceres, A. I., Catterall, W. A., Conner, A. C., … Zhu, M. (2023). The Concise Guide to PHARMACOLOGY 2023/24: Ion channels. *British Journal of Pharmacology*, *180*, S145–S222. https://doi.org/10.1111/bph.16181

Atack, J. R. (2009). $GABA_A$ Receptor α2/α3 subtype-selective modulators as potential nonsedating anxiolytics. In M. B. Stein & T. Steckler (Eds.), *Current topics in behavioral neuroscience* (Vol. 2) (pp. 331–360). Springer Verlag.

Atack, J. R. (2011). $GABA_A$ receptor subtype-selective modulators. I. α2/α3-selective agonists as non-sedating anxiolytics. *Current Topics in Medicinal Chemistry*, *11*(9), 1176–1202. https://doi.org/10.2174/156802611795371350

Atack, J. R., Hallett, D. J., Tye, S., Wafford, K. A., Ryan, C., Sanabria-Bohórquez, S. M., Eng, W. S., Gibson, R. E., Burns, H. D., Dawson, G. R., Carling, R. W., Street, L. J., Pike, A., De Lepeleire, I., Van Laere, K., Bormans, G., de Hoon, J. N., Van Hecken, A., McKernan, R. M., … Hargreaves, R. J. (2011). Preclinical and clinical pharmacology of TPA023B, a $GABA_A$ receptor α2/α3 subtype-selective partial agonis. *Journal of Psychopharmacology*, *25*(3), 329–344. https://doi.org/10.1177/0269881109354928

Barbanoj, M. J., Urbano, G., Antonijoan, R., Ballester, M. R., & Valle, M. (2007). Different acute tolerance development to EEG, psychomotor performance and subjective assessment effects after two intermittent oral doses of alprazolam in healthy volunteers. *Neuropsychobiology*, *55*(3–4), 203–212. https://doi.org/10.1159/000108379

Benke, D., Fritschy, J. M., Trzeciak, A., Bannwarth, W., & Möhler, H. (1994). Distribution, prevalence, and drug binding profile of gamma-aminobutyric acid type A receptor subtypes differing in the β-subunit variant. *Journal of Biological Chemistry*, *269*(43), 27100–27107. https://doi.org/10.1016/S0021-9258(18)47131-1

Bennett, G. J., & Xie, Y. K. (1988). A peripheral mononeuropathy in rat that produces disorders of pain sensation like those seen in man. *Pain*, *33*(1), 87–107. https://doi.org/10.1016/0304-3959(88)90209-6

Besson, M., Daali, Y., Di Lio, A., Dayer, P., Zeilhofer, H. U., & Desmeules, J. (2013). Antihyperalgesic effect of the $GABA_A$ ligand clobazam in a neuropathic pain model in mice: a pharmacokinetic-pharmacodynamic study. *Basic and Clinical Pharmacology and Toxicology*, *112*(3), 192–197. https://doi.org/10.1111/bcpt.12017

Breivik, H., Collett, B., Ventafridda, V., Cohen, R., & Gallacher, D. (2006). Survey of chronic pain in Europe: prevalence, impact on daily life, and treatment. *European Journal of Pain*, *10*(4), 287–333. https://doi.org/10.1016/j.ejpain.2005.06.009

Campbell, D. B. (1990). The use of kinetic-dynamic interactions in the evaluation of drugs. *Psychopharmacology*, *100*(4), 433–450. https://doi.org/10.1007/BF02243994

Curtis, M. J., Alexander, S. P. H., Cortese-Krott, M., Kendall, D. A., Martemyanov, K. A., Mauro, C., Panettieri, R. A. Jr., Papapetropoulos, A., Patel, H. H., Santo, E. E., Schulz, R., Stefanska, B., Stephens, G. J., Teixeira, M. M., Vergnolle, N., Wang, X., & Ferdinandy, P. (2025). Guidance on the planning and reporting of experimental design and analysis. *British Journal of Pharmacology*, *182*(7), 1413–1415. https://doi.org/10.1111/bph.17441

De Koninck, Y. (2007). Altered chloride homeostasis in neurological disorders: A new target. *Current Opinion in Pharmacology*, *7*(1), 93–99. https://doi.org/10.1016/j.coph.2006.11.005

Deglon, J., Thomas, A., Daali, Y., Lauer, E., Samer, C., Desmeules, J., Dayer, P., Mangin, P., & Staub, C. (2011). Automated system for on-line desorption of dried blood spots applied to LC/MS/MS pharmacokinetic study of flurbiprofen and its metabolite. *Journal of Pharmaceutical and Biomedical Analysis*, *54*(2), 359–367. https://doi.org/10.1016/j.jpba.2010.08.032

Di Lio, A., Benke, D., Besson, M., Desmeules, J., Daali, Y., Wang, Z. J., Edwankar, R., Cook, J. M., & Zeilhofer, H. U. (2011). HZ166, a novel $GABA_A$ receptor subtype-selective benzodiazepine site ligand, is antihyperalgesic in mouse models of inflammatory and neuropathic pain. *Neuropharmacology*, *60*(4), 626–632. https://doi.org/10.1016/j.neuropharm.2010.11.026

Dias, R., Sheppard, W. F., Fradley, R. L., Garrett, E. M., Stanley, J. L., Tye, S. J., Goodacre, S., Lincoln, R. J., Cook, S. M., Conley, R., Hallett, D., Humphries, A. C., Thompson, S. A., Wafford, K. A., Street, L. J., Castro, J. L., Whiting, P. J., Rosahl, T. W., Atack, J. R., … Reynolds, D. S. (2005). Evidence for a significant role of α3-containing $GABA_A$ receptors in mediating the anxiolytic effects of benzodiazepines. *The Journal of Neuroscience*, *25*(46), 10682–10688. https://doi.org/10.1523/JNEUROSCI.1166-05.2005

Ellinwood, E. H., Nikaido, A., & Heatherly, D. (1984). Diazepam: Prediction of pharmacodynamics from pharmacokinetics. *Psychopharmacology*, *83*(3), 297–298. https://doi.org/10.1007/BF00464800

Graham, D., Faure, C., Besnard, F., & Langer, S. Z. (1996). Pharmacological profile of benzodiazepine site ligands with recombinant $GABA_A$ receptor subtypes. *European Journal of Neuropsychopharmacology*, *6*(2), 119–125. https://doi.org/10.1016/0924-977x(95)00072-w

Khom, S., Baburin, I., Timin, E. N., Hohaus, A., Sieghart, W., & Hering, S. (2006). Pharmacological properties of $GABA_A$ receptors containing γ1 subunits. *Molecular Pharmacology*, *69*(2), 640–649. https://doi.org/10.1124/mol.105.017236

Knabl, J., Witschi, R., Hösl, K., Reinold, H., Zeilhofer, U. B., Ahmadi, S., Brockhaus, J., Sergejeva, M., Hess, A., Brune, K., Fritschy, J. M., Rudolph, U., Möhler, H., & Zeilhofer, H. U. (2008). Reversal of pathological pain through specific spinal $GABA_A$ receptor subtypes. *Nature*, *451*, 330–334. https://doi.org/10.1038/nature06493

Knabl, J., Zeilhofer, U. B., Crestani, F., Rudolph, U., & Zeilhofer, H. U. (2009). Genuine antihyperalgesia by systemic diazepam revealed by experiments in $GABA_A$ receptor point-mutated mice. *Pain*, *141*(3), 233–238. https://doi.org/10.1016/j.pain.2008.10.015

Lewter, L. A., Fisher, J. L., Siemian, J. N., Methuku, K. R., Poe, M. M., Cook, J. M., & Li, J. X. (2017). antinociceptive effects of a novel α2/α3-subtype selective $GABA_A$ receptor positive allosteric modulator. *ACS Chemical Neuroscience*, *8*(6), 1305–1312. https://doi.org/10.1021/acschemneuro.6b00447

Lewter, L. A., Woodhouse, K., Tiruveedhula, V., Cook, J. M., & Li, J. X. (2024). Antinociceptive effects of α2/α3-subtype selective $GABA_A$ receptor positive allosteric modulators KRM-II-81 and NS16085 in rats: Behavioral specificity. *Journal of Pharmacology and Experimental Theapeutics*, *391*(3), 389–398. https://doi.org/10.1124/jpet.123.002070

Li, J., Fish, R. L., Cook, S. M., Tattersall, F. D., & Atack, J. R. (2006). Comparison of in vivo and ex vivo [^{3}H]flumazenil binding assays to determine occupancy at the benzodiazepine binding site of rat brain $GABA_A$ receptors. *Neuropharmacology*, *51*(1), 168–172. https://doi.org/10.1016/j.neuropharm.2006.03.020

Lilley, E., Stanford, S. C., Kendall, D. E., Alexander, S. P., Cirino, G., Docherty, J. R., George, C. H., Insel, P. A., Izzo, A. A., Ji, Y., Panettieri, R. A., Sobey, C. G., Stefanska, B., Stephens, G., Teixeira, M., & Ahluwalia, A. (2020). ARRIVE 2.0 and the *British Journal of Pharmacology*: Updated guidance for 2020. *British Journal of Pharmacology*., *177*, 3611–3616. https://doi.org/10.1111/bph.15178

Lorenzo, L. E., Godin, A. G., Ferrini, F., Bachand, K., Plasencia-Fernandez, I., Labrecque, S., Girard, A. A., Boudreau, D., Kianicka, I., Gagnon, M., Doyon, N., Ribeiro-da-Silva, A., & De Koninck, Y. (2020). Enhancing neuronal chloride extrusion rescues α2/α3 $GABA_A$-mediated analgesia in neuropathic pain. *Nature Communications*, *11*(1), 869. https://doi.org/10.1038/s41467-019-14154-6

Louizos, C., Yanez, J. A., Forrest, M. L., & Davies, N. M. (2014). Understanding the hysteresis loop conundrum in pharmacokinetic/pharmacodynamic relationships. *Journal of Pharmacology and Pharmaceutical Sciences*, *17*(1), 34–91. https://doi.org/10.18433/J3GP53

Löw, K., Crestani, F., Keist, R., Benke, D., Brünig, I., Benson, J. A., Fritschy, J. M., Rülicke, T., Bluethmann, H., Möhler, H., & Rudolph, U. (2000). Molecular and neuronal substrate for the selective attenuation of anxiety. *Science*, *290*(5489), 131–134. https://doi.org/10.1126/science.290.5489.131

Luurila, H., & Olkkola, K. T. (1996). Pharmacokinetic-pharmacodynamic modelling of zopiclone effects on human central nervous system. *Pharmacology and Toxicology*, *78*(5), 348–353. https://doi.org/10.1111/j.1600-0773.1996.tb01387.x

Neumann, E., Cramer, T., Acuña, M. A., Scheurer, L., Beccarini, C., Luscher, B., Wildner, H., & Zeilhofer, H. U. (2024). γ1 $GABA_A$ receptors in spinal nociceptive circuits. *The Journal of Neuroscience*, *44*(41), e0591242024. https://doi.org/10.1523/JNEUROSCI.0591-24.2024

Neumann, E., Kupfer, L., & Zeilhofer, H. U. (2021). The α2/α3$GABA_A$ receptor modulator TPA023B alleviates not only the sensory but also the tonic affective component of chronic pain in mice. *Pain*, *162*(2), 421–431. https://doi.org/10.1097/j.pain.0000000000002030

Nickolls, S., Mace, H., Fish, R., Edye, M., Gurrell, R., Ivarsson, M., Pitcher, T., Tanimoto-Mori, S., Richardson, D., Sweatman, C., Nicholson, J., Ward, C., Jinks, J., Bell, C., Young, K., Rees, H., Moss, A., Kinloch, R., & McMurray, G. (2011). A Comparison of the α2/3/5

Selective positive allosteric modulators L-838,417 and TPA023 in preclinical models of inflammatory and neuropathic pain. *Advances in Pharmacological Sciences*, *2011*, 608912. https://doi.org/10.1155/2011/608912

Paul, J., Yévenes, G. E., Benke, D., Di Lio, A., Ralvenius, W. T., Witschi, R., Scheurer, L., Cook, J. M., Rudolph, U., Fritschy, J. M., & Zeilhofer, H. U. (2014). Antihyperalgesia by α2-$GABA_A$ receptors occurs via a genuine spinal action and does not involve supraspinal sites. *Neuropsychopharmacology*, *39*(2), 477–487. https://doi.org/10.1038/npp.2013.221

Paul, J., Zeilhofer, H. U., & Fritschy, J.-M. (2012). Selective distribution of $GABA_A$ receptor subtypes in mouse spinal dorsal horn neurons and primary afferents. *Journal of Comparative Neurology*, *520*, 3895–3911. https://doi.org/10.1002/cne.23129

Percie du Sert, N., Hurst, V., Ahluwalia, A., Alam, S., Avey, M. T., Baker, M., Browne, W. J., Clark, A., Cuthill, I. C., Dirnagl, U., Emerson, M., Garner, P., Holgate, S. T., Howells, D. W., Karp, N. A., Lazic, S. E., Lidster, K., MacCallum, C. J., Macleod, M., … Würbel, H. (2020). The ARRIVE guidelines 2.0: Updated guidelines for reporting animal research. *PLoS Biology*, *18*(7), e3000410. https://doi.org/10.1371/journal.pbio.3000410

Pirker, S., Schwarzer, C., Wieselthaler, A., Sieghart, W., & Sperk, G. (2000). $GABA_A$ receptors: Immunocytochemical distribution of 13 subunits in the adult rat brain. *Neuroscience*, *101*, 815–850. https://doi.org/10.1016/s0306-4522(00)00442-5

Ralvenius, W. T., Acuña, M. A., Benke, D., Matthey, A., Daali, Y., Rudolph, U., … Besson, M. (2016). The clobazam metabolite N-desmethyl clobazam is an α2 preferring benzodiazepine with an improved therapeutic window for antihyperalgesia. *Neuropharmacology*, *109*, 366–375. https://doi.org/10.1016/j.neuropharm.2016.07.004

Ralvenius, W. T., Benke, D., Acuña, M. A., Rudolph, U., & Zeilhofer, H. U. (2015). Analgesia and unwanted benzodiazepine effects in point-mutated mice expressing only one benzodiazepine-sensitive $GABA_A$ receptor subtype. *Nature Communications*, *6*, 6803. https://doi.org/10.1038/ncomms7803

Ralvenius, W. T., Neumann, E., Pagani, M., Acuña, M. A., Wildner, H., Benke, D., Fischer, N., Rostaher, A., Schwager, S., Detmar, M., Frauenknecht, K., Aguzzi, A., Hubbs, J. L., Rudolph, U., Favrot, C., & Zeilhofer, H. U. (2018). Itch suppression in mice and dogs by modulation of spinal α2 and α3$GABA_A$ receptors. *Nature Communications*, *9*(1), 3230. https://doi.org/10.1038/s41467-018-05709-0

Reichl, S., Augustin, M., Zahn, P. K., & Pogatzki-Zahn, E. M. (2012). Peripheral and spinal GABAergic regulation of incisional pain in rats. *Pain*, *153*(1), 129–141. https://doi.org/10.1016/j.pain.2011.09.028

Rudolph, U., Crestani, F., Benke, D., Brünig, I., Benson, J. A., Fritschy, J. M., Martin, J. R., Bluethmann, H., & Möhler, H. (1999). Benzodiazepine actions mediated by specific γ-aminobutyric $acid_A$ receptor subtypes. *Nature*, *401*(6755), 796–800. https://doi.org/10.1038/44579

Sieghart, W., & Savic, M. M. (2018). International union of basic and clinical pharmacology. CVI: $GABA_A$ receptor subtype- and function-selective ligands: Key issues in translation to humans. *Pharmacological Reviews*, *70*(4), 836–878. https://doi.org/10.1124/pr.117.014449

van Amerongen, G., Siebenga, P. S., Gurrell, R., Dua, P., Whitlock, M., Gorman, D., Okkerse, P., Hay, J. L., Butt, R. P., & Groeneveld, G. J. (2019). Analgesic potential of PF-06372865, an α2/α3/α5 subtype-selective $GABA_A$ partial agonist, in humans. *British Journal of Anaesthesiology*, *123*(2), e194–e203. https://doi.org/10.1016/j.bja.2018.12.006

van Rijnsoever, C., Tauber, M., Choulli, M. K., Keist, R., Rudolph, U., Mohler, H., Fritschy, J. M., & Crestani, F. (2004). Requirement of α5-$GABA_A$ receptors for the development of tolerance to the sedative action of diazepam in mice. *Journal of Neuroscience*, *24*(30), 6785–6790. https://doi.org/10.1523/JNEUROSCI.1067-04.2004

Werynska, K., Neumann, E., Cramer, T., Ganley, R. P., Gingras, J., & Zeilhofer, H. U. (2023). A phosphodeficient α3 glycine receptor mutation alters synaptic glycine and GABA release in mouse spinal dorsal horn neurons. *Journal of Physiology*, *601*, 4121–4133.

Wingrove, P. B., Thompson, S. A., Wafford, K. A., & Whiting, P. J. (1997). Key amino acids in the gamma subunit of the γ-aminobutyric acidA receptor that determine ligand binding and modulation at the benzodiazepine site. *Molecular Pharmacology*, *52*(5), 874–881. https://doi.org/10.1124/mol.52.5.874

Wright, C. E., Sisson, T. L., Fleishaker, J. C., & Antal, E. J. (1997). Pharmacokinetics and psychomotor performance of alprazolam: concentration-effect relationship. *Journal of Clinical Pharmacology*, *37*(4), 321–329. https://doi.org/10.1002/j.1552-4604.1997.tb04309.x

Zeilhofer, H. U., Benke, D., & Yévenes, G. E. (2012). Chronic pain states: pharmacological strategies to restore diminished inhibitory spinal pain control. *Annual Reviews in Pharmacology and Toxicology*, *52*, 111–133. https://doi.org/10.1146/annurev-pharmtox-010611-134636

Zeilhofer, H. U., Ralvenius, W. T., & Acuna, M. A. (2015). Restoring the spinal pain gate: $GABA_A$ receptors as targets for novel analgesics. *Advances in Pharmacology*, *73*, 71–96. https://doi.org/10.1016/bs.apha.2014.11.007

Zeilhofer, H. U., & Zeilhofer, U. B. (2008). Spinal dis-inhibition in inflammatory pain. *Neuroscience Letters*, *437*(3), 170–174. https://doi.org/10.1016/j.neulet.2008.03.056

How to cite this article: Neumann, E., Popa, M. O., Elvers, K. T., Oyama, M., Ulrich, D., Hanley, M., Feng, G. J., Hathaway, T., Ralvenius, W. T., Grampp, T., Benke, D., Atack, J. R., & Zeilhofer, H. U. (2026). A PK/PD study on antihyperalgesia by an α2/3-$GABA_A$ receptor PAM in mice: Lack of tolerance liability and potential involvement of γ1-$GABA_A$ receptors. *British Journal of Pharmacology*, 1–17. https://doi.org/10.1111/bph.70301